Modelling the fire propagation from the fuel bed to the lower canopy of ornamental species used in wildland–urban interfaces

L. Terrei, A. Lamorlette, Anne Ganteaume

Author-produced version of the article published in International Journal of Wildland Fire, 28, 2, 113-126.
The original publication is available at http://www.publish.csiro.au/wf/WF18090
DOI: 10.1071/WF18090

Modelling the fire propagation from the fuel bed to the lower canopy of ornamental species used in wildland–urban interfaces

L. Terrei[A,B], *A. Lamorlette*[A] *and A. Ganteaume*[B,C]

[A]IRSTEA RECOVER-EMR, 3275 route de Cézanne, 13182 Aix-en-Provence Cedex 5, France.

[B] M2P2 UMR7340 Centrale Marseille Plot 6, 38 rue Joliot-Curie, 13451 Marseille, France.

[C]Corresponding author. Email: anne.ganteaume@irstea.fr

Abstract. South-eastern France is strongly affected by wildfires mostly occurring in the wildland–urban interfaces (WUIs). A WUI fire is often initiated in dead surface fuel, then can propagate to shrubs and trees when the lower canopy is close to (or touches) the ground. Whereas a previous study assessed the fire propagation from the fuel bed to the lower canopy of different species used as ornamental vegetation in this region, the objectives of the current work consisted of checking if the modelling of this fire propagation was possible using WFDS (Wildland–Urban Interface Fire Dynamical Simulator) in comparing experimental and modelling results. Experimental and modelling constraints (i.e. branch geometric definition, branch motion due to convection) showed differences in some of the recorded data (such as time to ignition, ignition temperature, mass loss and maximum temperature), but comparisons of variation in mass loss and temperature over time showed that modelling the fire propagation at the scale of a branch was possible if the branch fuel-moisture content remained lower than 25%. For both experiments and modelling, the ranking of species according to their branch flammability highlighted identical groups of species.

Additional keywords: fuel flammability, WFDS, WUI vegetation.

In WUI, a fire is often initiated in litter, then can propagate to the plant canopy when its lower part is close to the ground. Comparing experimental and numerical results showed that, mostly, modelling the fire propagation at the scale of a branch was possible using WFDS but only if the branch moisture content remained lower than 25%. Improvements are needed to use higher moisture contents in the modelling.

Introduction

Around the world, global concerns about the impact of wildland fires are increasingly focusing on the wildland–urban interface (WUI) where their occurrence, mostly human-caused, is high and where they greatly affect life and properties (Etlinger and Beall 2004; Syphard *et al*. 2007). These fires regularly destroy structures when fuel and weather are conducive to fire and WUIs are now considered as priority areas for controlling wildfires. South-eastern France, where the current work took place, is particularly affected by this fire issue (on average, 182 fires and 1111 ha burned per year between 2012 and 2016) as 47% of the ignitions occur in the WUI representing only 15% of this zone (Ganteaume and Long-Fournel 2015).

The expansion of WUIs, together with the high proportion of fire ignitions, are factors that require the study of the flammability of vegetation located around structures and, in particular, the ornamental hedges delimiting each property that provide a horizontal fuel continuity. Indeed, this ornamental vegetation can propagate fire from forest to buildings, potentially carrying it from structure to structure. Previous works assessed the flammability of some of the most common ornamental species found in SE France, taking into account dead surface fuel (fuel bed) and live leaves (Ganteaume *et al*. 2013*a*, 2013*b*; Ganteaume 2018), but also the fire propagation from the fuel bed to the lower canopy (Ganteaume *et al*. 2016). Based on these works, modelling this fire propagation, besides saving a considerable amount of time compared with the time-consuming laboratory experiments, would provide a complementary perspective in validating the modelling results. Previous works on the modelling of fire propagation used WFDS (Wildland–urban interface Fire Dynamic Simulator) for their simulations (e.g. Mell *et al*. 2007, 2009). This model is an extension of FDS (Fire Dynamic Simulator; McGrattan *et al*. 2013), which is mostly used in fire-safety engineering and includes a multiphasic model (i.e. model that is based on balance equations for both the solid and the fluid phases, considering mass, heat and momentum transfer from a phase to another) as in Grishin (1997) and in Morvan and Dupuy (2001) to simulate vegetation fires. WFDS was previously used to model fire propagation at different scale: forest fire (Hoffman *et al*. 2012), Australian grassland fires (Mell *et al*. 2007), trees to study the vertical flame spread (Mell *et al*. 2010). Simulating fire propagation in a pine fuel bed (Perez-Ramirez *et al*. 2017) or in entire Douglas-firs (Mell *et al*. 2009) as well as comparing WFDS numerical and experimental results were also previously performed.

However, the vegetation used in WUIs can differ from the wildland vegetation (i.e. forest or shrubland), especially regarding their structure and spatial distribution in these areas. Moreover, WUI fuels are inherently inhomogeneous in type with a mix of structural fuels, native, as well as exotic species (the two latter comprising the ornamental vegetation). Currently, the knowledge on fire propagation within this ornamental vegetation is poor, regardless of the scale. Modelling fire propagation at large scale using a multiphasic model, such as WFDS, has already been attempted (e.g. Hoffman *et al*. 2012; Ziegler *et al*. 2017), in contrast, modelling at fine scale has been scarcely studied. Among the few studies, some were carried out on surface fuel (Bufacchi *et al*. 2016; Perez-Ramirez *et al*. 2017) or attempted to model surface to crown-fire transition (Castle *et al*. 2013; Castle 2015). The ignition sources used also varied from one work to another, using controlled ignition sources in the modelling, such as burners (Overholt *et al*. 2014) or controlled radiative heat sources (El Houssami 2016). The multiphasic model has already been tested at this scale (El Houssami *et al*. 2016, 2018) but numerical studies of a branch ignited by a flame front generated by a burning fuel bed have not been conducted yet. It was interesting to evaluate how WFDS would perform at this fine scale (i.e. branch scale) and to check whether the simulation of the fire propagating from the fuel bed to the lower canopy of different ornamental species was possible using this model. Indeed, this configuration

represented the first step in understanding the vertical fire propagation as it occurs during spot fires, which are frequent during WUI fires. The objectives of this work were to compare numerical and experimental results in order to assess the accuracy of the modelling using WFDS and to pinpoint possible limitations which could be tackled in future works.

Material and methods

Species studied

The four species studied are among the most commonly found in the WUI of SE France: the Italian cypress (*Cupressus sempervirens*, L.) characterised by its scale leaves, the oleander (*Nerium oleander*, L.), the Japanese spindle (*Euonymus japonicus*, Thunb.) and the cotoneaster (*Cotoneaster franchetti*, Bois). The two former species are also native to other Mediterranean areas, such as Italy and Greece. The flammability of these four species has already been evaluated at the fuel bed and leaf scales in laboratory conditions (Ganteaume *et al*. 2013*a*, 2013*b*, Ganteaume 2018).

Modelling with WFDS

Overview

Modelling was carried out using WFDS, an extension of FDS6 (Fire Dynamical Simulator, ver. 6, rev. 9977, Gaithersburg, Maryland, USA), developed by National Institute of Standards and Technology (NIST) for the three-dimensional prediction of fire behaviour. This software uses numerical simulation to solve the equations of combustion, heat transfer and thermal degradation of plant fuels (Mell *et al*. 2009). Version 6 of FDS has been used in this study, as it had been validated in Mell *et al*. (2009). The set of equations of the multiphase model and the numerical methods of this version were thus considered as fully reliable. The solution method uses the LES (Large Eddy Simulation) to solve the mass equations, the momentum and the energy, with a low-Mach number formulation. Vegetation is composed of elements that are thermally thin (Lamorlette and Candelier 2015) and optically black (the emissivity of 0.9 characterises thin natural vegetation; Monod *et al*. 2009) as it is mandatory to derive the multiphase model equations, as presented in Grishin (1997). The thermally thin hypothesis is commonly used in fire-propagation models involving fine natural fuels, although debatable, in particular for the combustion of plants (Lamorlette and Candelier 2015).

The following constraints of WFDS led to the modification of the experimental device used in a previous work (Ganteaume *et al*. 2016):

- The fuel moisture content (FMC) has a very important role in plant flammability, both in experiments and WFDS modelling (Bufacchi *et al*. 2016). Research has also shown that modelling burning vegetation that presents high moisture content can distance the results from reality (El Houssami *et al*. 2016). In the current work, a FMC range lower than 25% was chosen to avoid this problem. This aspect will be discussed later in the article.

• WFDS was initially used to model forest fires, thus at a much larger scale than a single branch. In the modelling, the plants were represented as simple geometric shapes (e.g. cone, cylinder, rectangle), with a uniform fuel distribution. The volume of vegetation in the current work is smaller compared with the former studies using WFDS but it has to be at least of the same magnitude as a representative elementary volume of the tree (Bear and Bachmat 2012).

This study was a first step in estimating the ability of WFDS to model fire propagation at this scale, using a 'standard' fuel bed characterised by a more homogeneous composition and structure than the one used in the previous work (i.e. litter samples collected undisturbed underneath the hedge in Ganteaume *et al*. 2016). Indeed, the fuel bed chosen to generate a flame front was not the undisturbed fuel bed of the species studied (highly heterogeneous in terms of components and compactness) but an excelsior fuel bed instead. This type of fuel bed is commonly used in laboratory experiments because its combustion occurs easily and without residue. Moreover, the flame front generated after ignition is homogeneous, thus lessening the flame instabilities during the burning. The fuel-bed characteristics used in the modelling (e.g. thickness) were the same as those used in the experiments (Table 1). The spatial domain used in these simulations measured 60 × 30 × 00 cm according to $\vec{x}$, $\vec{y}$, $\vec{z}$ coordinates and the resolution was 1 cm in $\vec{x}$, $\vec{z}$ direction and 0.5 cm in the $\vec{y}$ direction for a numerical grid of 60 × 60 × 100 cells. The boundary conditions were modelled by 'VENT' with parameter 'OPEN' (that denotes a passive opening to the outside without any obstacles or solid wall) for both horizontal and vertical surfaces. No slope or wind conditions were imposed for this study and the total simulation time was 70 s (but required 8 h of computation time).

Designing the branch shape

The precise geometric definition of a branch using WFDS was not possible due to the diversity of branch shapes according to species but also due to the limited geometric shapes available in the software. Some studies accurately modelled the shrub geometry with FUEL3D software (Fuel 3D Inc., Greenville, USA) and have highlighted the importance of wood heterogeneity in the fire behaviour (Parsons *et al*. 2011; Prince *et al*. 2014). Generally, in WFDS, the branch modelled by a single cylinder is in good agreement with the experiments (Overholt *et al*. 2014), but this modelling was not realistic enough. So, the branch was built from a multitude of small cylinders that, once put together, better represented the shape of the branch of each species studied. For this work, a specific branch geometry must be considered for each species (Fig. 1) and its dimensions have to be of the same order as those of the branches burned in the laboratory to allow comparisons. The cylinders used in the modelling represented a homogeneous medium, equivalent to both branches and leaves. In other words, these cylinders defined containers in which the leaves and branches are located.

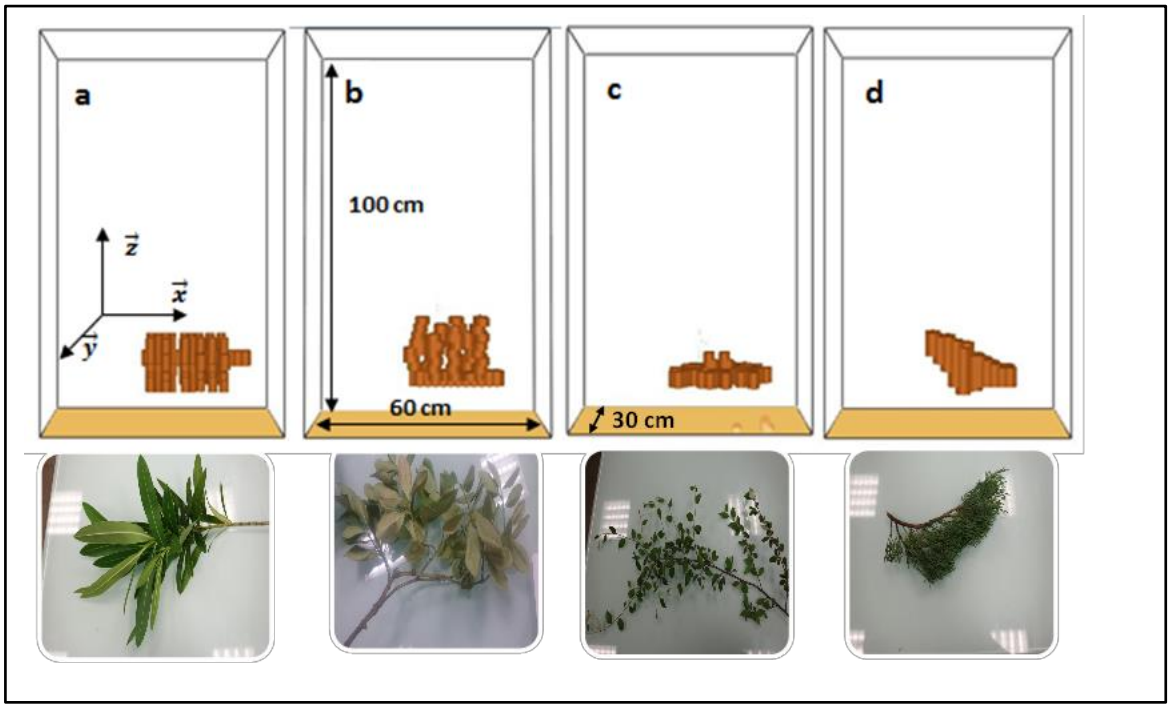

Figure 1: Geometric definition of a branch for the four ornamental species and the experimental fuels used: (a) oleander, (b) spindle, (c) cotoneaster, (d) cypress.

Input parameters

All parameters used in the numerical branch burning (i.e. branch and thermocouple position, fuel bed ignition) as well as the input parameters (i.e. leaf moisture content, char fraction, branch bulk density and leaf surface-to-volume ratio) were based on measurements made during the laboratory experiments (Table 2).

Experiments

For each species, the experiments took place according to four steps: branch sampling, branch drying, branch calibration and branch burning (in laboratory conditions).

Excelsior fuel bed

The fuel bed underneath the branch, characterising the species in terms of structure and composition, has a very important role in flame propagation. However, for these undisturbed fuel beds, the flame front generated was not homogeneous (litter mass varying from one sample to another and its composition being heterogeneous when collected undisturbed; see Ganteaume *et al*. 2016). The excelsior fuel bed allowed a simplification in both experiments and modelling and is regularly used to model surface fuel in burning experiments (Dickinson *et al*. 2013; Cobian-Iñiguez *et al*. 2017). This fuel is highly flammable and the flame front is more constant during the burning process than with the undisturbed litter bed. Using the same fuel bed for all species also allowed the setting of a constant

fuel-bed mass that was evenly distributed on the fire bench. According to preliminary burning tests the Excelsior fuel bed presented a depth of 1.5 cm (resulting of the standardised compaction of the samples in order to get similar fuel depths), for a total mass of 15 g, distributed over the dedicated 30 × 40-cm surface area (negligible variations could be due to the texture of the excelsior, i.e. intertwined thin strips).These fuel-bed characteristics (Table 1) were selected in order to generate mean flame heights of 23.9 cm (±3.3 cm), which were capable of reaching the branch. The location of the branch in the experiment and in the modelling was, therefore, fixed at 10 cm above the fuel bed as this height was representative of the height of the lower canopy commonly found in ornamental hedges (Ganteaume *et al*. 2016).

Branch sampling

The live branches were collected directly from the trees at Le Tholonet (Bouches-du-Rhône, SE France), from April to June 2017. For each species, the samples were collected at the same time in order to avoid differences in fuel-moisture content within a species. Branches were collected on mature plants, avoiding the newly formed tissues so that they did not differ in terms of structure and size (especially regarding the leaves).

Branch drying

Regardless of species, the branch moisture content was always higher than 100% at the moment of the sampling, so air-drying the branches before the burning experiments was necessary to be able to compare the results with those obtained with WFDS, as the multiphasic modelling seems to require low fuel-moisture content, as shown in El Houssami (2016). The branches were air-dried in a closed chamber (a powered down drying-oven) in order to avoid sudden variations of dehydration due to the variation of climatic conditions (especially during dry windy episodes). The branch dehydration was calculated daily to accurately check the sample moisture-content variation. FMC was calculated according to Eqn 1, by oven-drying for 48 h at 60°C a sub-sample of the branch (only composed of leaves), previously weighed (M_F) . After the oven-drying, the sub-sample was weighed again to obtain the dry weight (M_D). Because of FMC higher than 100% at the time of sampling, air-drying took several days before reaching the adequate FMC (<25%).

$$FMC = \frac{M_F - M_D}{M_D} \times 100 \quad (1)$$

Branch calibration

As required in WFDS, the branch bulk density (BD) has to be representative of at least an elementary volume of the tree to be able to compare numerical and experimental data. Branch samples were weighed, then trimmed (some leaves and twigs were removed when needed; Fig. 2) in order to get samples as homogeneous as possible, mostly in terms of geometry and bulk density (Table 2). Except for cotoneaster, most of the branch dry weight was due to the leaves. To determine the bulk

density, each branch had to be approximated by a geometric shape (a cone for cypress, a cylinder for oleander, a rectangle for spindle and cotoneaster). Then, the branch mass was divided by the volume of the geometric form, giving the bulk density in kilograms per cubic metre (Table 2).

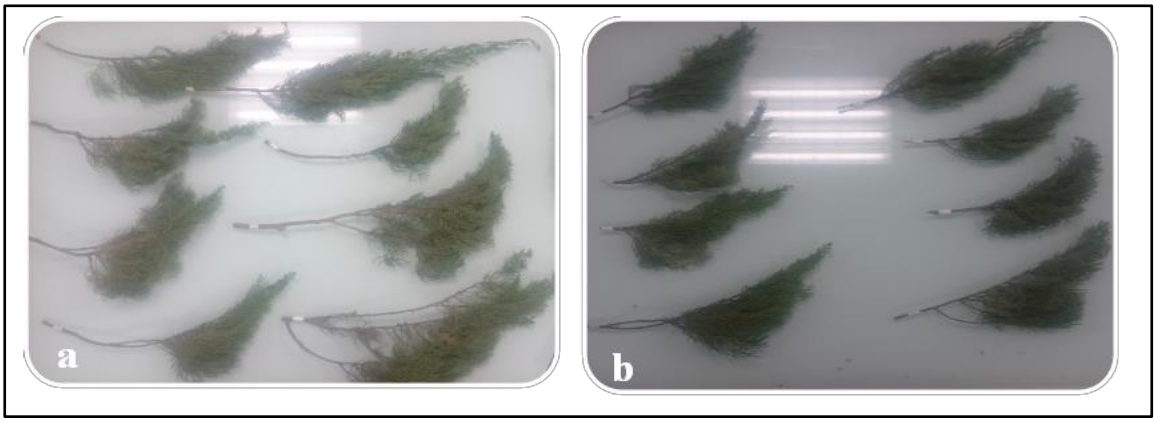

Figure 2: Branch calibration: cypress samples before (a) and after (b) trimming.

Burning experiments

The experimental device, based on a previous work (Ganteaume *et al*. 2016), was adapted according to the limitations due to the modelling (Fig. 3). Preliminary comparisons between numerical and experimental data were performed burning only fuel beds, recording mass loss and temperature variations over time. Then, the branch was placed on a weighing scale to record the branch mass loss during burning, centred with its lowest part 10 cm above the fuel bed (slight variations could be due to the branch shape). The distance between the fuel-bed line ignition and the branch was set at 15 cm to allow the flame front to fully develop as it was designed and tested in Ganteaume *et al*. (2016). For each species, the angle between the branch and the fuel bed in the numerical simulation was the same as the angle between the branch and the ground measured in the field. The fuel bed was ignited by a line ignition, using a cotton string soaked with ethanol in order to generate a flame front as linear and constant as possible.

The experimental device was also composed of three type-k thermocouples (Omega Engineering, Stamford, CT, USA), two placed around the branch and one located 1 cm above (Fig. 3, Table 3). This type of thermocouple, with a low diameter (0.25 mm), presented a very low inertia in the recording of temperature (5 measurements per second). Thermocouples were purposely located around the branch in order to avoid distorting mass measurements if the branch moved. The thermocouples were plugged to a CR800 Campbell data logger (Campbell Scientific Inc., Logan, UT, USA) to record the variation of temperatures during the branch burning experiments. The coordinates ($\vec{x}$, $\vec{y}$, $\vec{z}$) of these thermocouples were noted before each test in order to place the temperature sensors at the same location in WFDS. Data were measured using the software PC200 (Campbell Scientific Inc., Logan, UT, USA), with a 5-Hz acquisition frequency.

A Canon video camera EOS 6D (WG) was used to record the burning tests and a thermal camera (model:FLIR-T62101, number: 62114019, Boston, MA, USA) was added to more precisely study the location and ignition temperature of the branch, using the FLIR software (flir_researchir_max_4.30.1_(4.30.1.70)).

During the experiments, the branch mass loss was measured using a precision Mettler Toledo scale (model: XSR10002S, number: B748058617) with an accuracy of 0.01 g. The preliminary burning tests showed that samples of excelsior fuel bed were fully burned (100% mass loss); thus the fuel bed mass loss was not recorded during the current experiment.

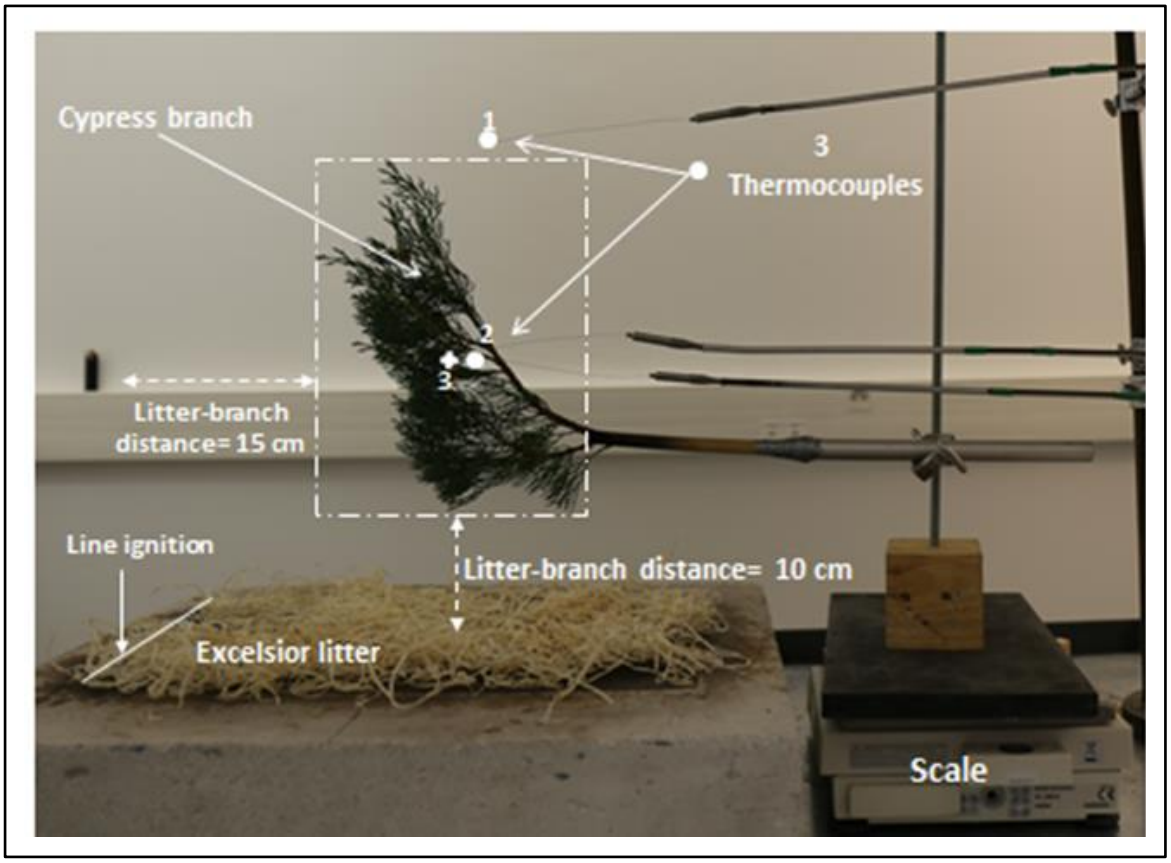

Figure 3: Experimental device (fire bench) used for the burning experiments (here for a cypress branch).

According to Anderson (1970) and Martin *et al.* (1993), the fuel flammability was characterised by four components: (i) ignitability, characterised in the current work by the branch time to ignition (TTI, s), which corresponded to the time necessary for the appearance of a flame and by the ignition temperature (IgT, °C), which was the temperature emitted when the flame appeared, (ii) consumability, characterised by the mass loss rate (MLR, g s^{-1}), (iii) sustainability, characterised by the branch flaming duration (FD, s) between the branch ignition and the end of its flaming combustion, and (iv) combustibility, characterised by the maximum temperature emitted by the flames and recorded by the three thermocouples ($MaxT_1$, $MaxT_2$ and $MaxT_3$, °C) and by the flame rate of

spread (ROS, cm s^{-1}) in the branch, which was measured by recording the time required by the flames to cover the 20 cm of the branch length. This variable refers to the local horizontal spreading of the flame front, which is often simply called rate of spread among the different common flammability variables, as in Anderson (1970), for instance. Once the fuel bed was ignited and as soon as the flame front reached the branch, a timer was switched on to record TTI and FD; the timing-specific measurements were made by visual inspections as it is the case in these types of experiments. The number of replicates per species is given in Table 2.

Calculation of model outputs

In the experiments, the ignition and the flaming duration were measured or can be deduced from the mass loss over time. In WFDS, these two parameters were initially observed in the visualization program Smokeview vers. 6 (NIST, Gaithersburg, Maryland, USA) used to display the output of FDS simulations, thanks to iso-surfaces of heat release rate per unit volume. TTI as well as FD were mainly deduced from the mass loss over time. Indeed, the sudden drop in mass loss was related to the ignition onset and, as soon as the flame disappeared, the mass loss became constant and FD was deduced from TTI and branch-extinction time.

Data analysis

The four ornamental species were ranked according to their branch flammability, taking into account the flammability variables (TTI, FD, MLR, ROS, IgT, MaxT) measured during the burning experiments and modelled by WFDS, using hierarchical cluster analysis (Ward method, based on squared Euclidian distance; Wishart 1969) in order to compare the ranking of species obtained with experimental and numerical data. This analysis was used to group species into categories of flammability in such a way that two species from the same cluster were more similar than two species from different clusters regarding their flammability variables. Principal Component Analyses were performed on the numerical and experimental datasets to highlight the flammability variables that characterised the fire behaviour of each species. These analyses were performed using Statgraphics Centurion XV (StatPoint Technologies, Inc., Warrenton, Virginia, USA).

Results

Comparisons of experimental and numerical flammability variables characterising the flammability of the four species studied

Numerical and experimental flammability results were compared for the four species studied (Table 4). For both numerical and mean experimental values, cotoneaster presented the longest FD (34 and 44 s respectively) and the shortest TTI (17 s) in contrast to cypress that took at least 30 s to ignite and that also had the lowest ignition temperature (248°C) but the highest experimental MLR (0.37 g s^{-1}). Oleander presented the highest maximum temperatures (except for the simulated $MaxT_1$) and

numerical MLR and ROS, whereas cypress and spindle presented the highest experimental values respectively (Table 4).

Considering the associated standard deviation, in some cases, mean experimental and simulated values were in a good agreement. When the numerical values were underestimated (value lower than mean – standard deviation) or overestimated (value higher than mean + standard deviation), the magnitude of the difference between numerical and experimental values is given in Table 4. TTi and $MaxT_3$ were the flammability variables the best predicted (except for cypress and spindle, which were overestimated, +19 and +16% respectively). Numerical ROS was overestimated regardless of species (ranging from +15% for spindle to +47% for oleander) in contrast to numerical FD which was underestimated (ranging from –23% for cotoneaster to –46% for cypress and oleander) for all species but spindle. Regarding MLR and $MaxT_1$, simulated values were overestimated or underestimated depending on species (except MLR for spindle and $MaxT_1$ for oleander), magnitudes ranging from +20 and –11% for cotoneaster to –77% for oleander (regarding MLR) and +30% for spindle (regarding $MaxT_1$). $MaxT_2$ was correctly predicted for cypress and cotoneaster but the numerical values were overestimated for spindle (+22%) and underestimated for oleander (–11%).

Prediction of the mass loss over time

WFDS modelled the fuel-bed mass loss during the burnings using the same characteristics as in the experiments and the numerical and experimental data were compared (Fig. 4). The 0.5-g difference highlighted between the experimental and the numerical initial masses could be explained by the mass of the cotton string soaked with ethanol used to generate the flame front, which was not represented in the modelling. On the whole, the numerical mass loss over time was in a good agreement with the range of experimental values which means that the burning time was also well predicted for the fuel-bed burnings.

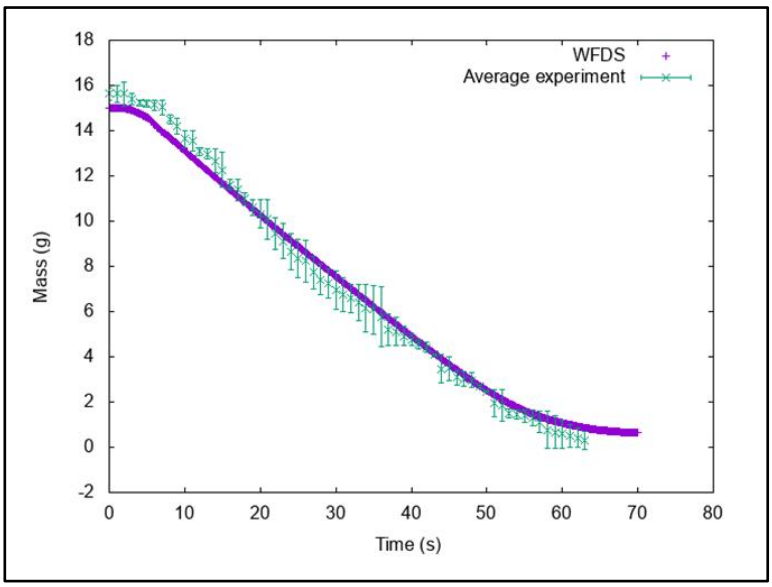

Figure 4: Comparison of fuel bed mass loss between WFDS and experiments (mean values n= 2).

The branch mass loss over time was modelled according to different values of branch moisture content (FMC = 10, 15 and 25%; Fig. 5). For FMC = 10%, the mass decreased faster than for FMC = 15% simply because the moisture content was lower so the branch ignition was faster. For FMC = 25%, the mass loss hardly varied showing that the branch burned only slightly, entailing just a little mass loss. This FMC, however, remained very low compared with those calculated directly after the branch collection in the field (>100%). Yet, the vegetation capacity to burn with high moisture content has been demonstrated in several works (i.e. Chuvieco *et al*. 2009; Ganteaume *et al*. 2016). This result confirmed the necessary limitation in terms of branch moisture content when comparing the experiments to the modelling regarding the mass loss since, in the experiments, the branch actually burned for FMC = 25%.

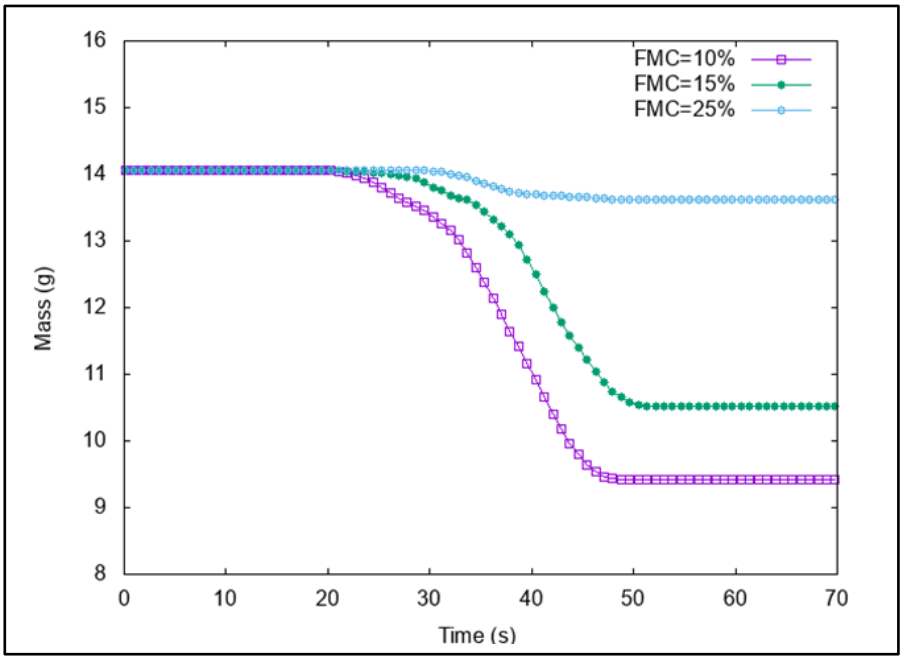

Figure 5: Modeling the mass loss of the spindle branch during the burning according to different FMCs.

The numerical and mean experimental data obtained for the branch mass loss were compared for the four ornamental species (Fig. 6). Regardless of species, the woody part of the branch did not take part to the mass loss as it did not burn. According to visual observations, all the curves were similar over time till the end of the burning (highlighting a correct prediction of the burning duration). For oleander (Fig. 6*a*), the decrease in mass loss occurred at 35 s in both experiments and modelling but, in the experiments, the decrease occurred more regularly than in the modelling (which showed a strong decrease after 40 s). For cypress (Fig. 6*a*), the numerical decrease in mass loss occurred 7 s later than in the experiments, meaning that the branch ignited sooner in the latter case. For cotoneaster and spindle, the numerical and experimental mass losses were in a good agreement, the values decreasing at the same time (~30 s), meaning that the numerical and experimental branch time to ignition matched (Fig. 6*b*).

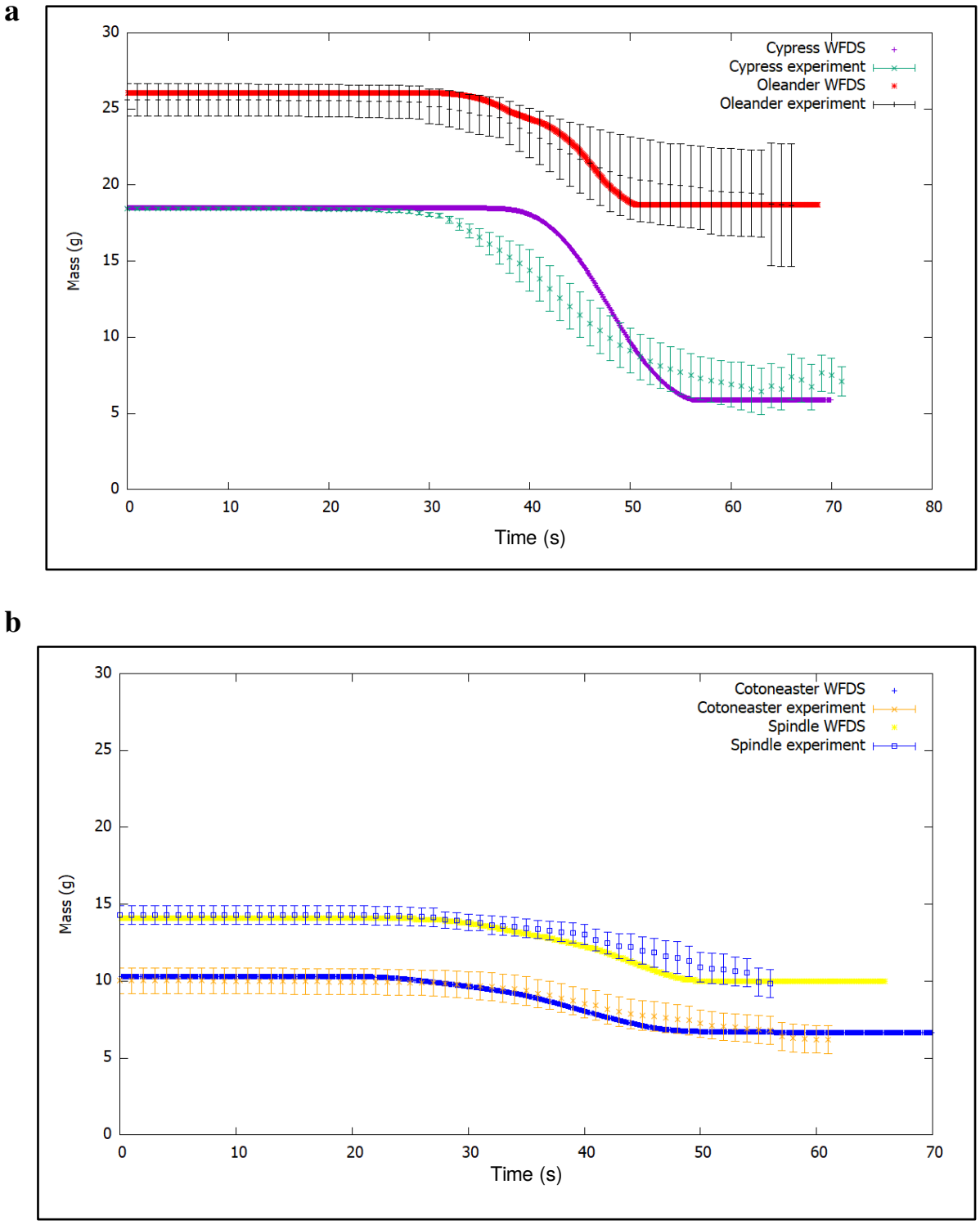

Figure 6: Comparison of the mass loss over time measured during the experiments (mean values) and in the WFDS modeling for (a) cypress (n= 8) and oleander (n= 3), (b) spindle (n= 7) and cotoneaster (n= 5).

Prediction of the temperature variation over time

The temperature variation during the fuel-bed burnings recorded at three different locations above the fuel bed (2.5, 3 and 15 cm) were compared between the modelling and the experiments (Fig. 7). On the whole, the numerical variation in temperatures was in a good agreement with the experimental data highlighting, in both cases, a concomitant increase in temperature (at 30 s in Fig. 7*a* and at 12 s in Fig. 7*b*). Comparing the two curves, a difference of 100°C was highlighted in the peak temperature, the experimental values being higher (Fig. 7*a*, *b*). For these two first configurations, the decrease in temperatures was longer in the experiments (5-s offset). Besides this longer decrease in temperature, when the sensor was placed at the highest position above the fuel bed (15 cm), there was a 5-s offset in the peak temperature, which showed a plateau at 300°C in the experimental data and a second peak reaching 200°C at 35 s in the simulation (Fig. 7*c*). In the simulation, the main peak of temperature was 100°C higher than in the experiments.

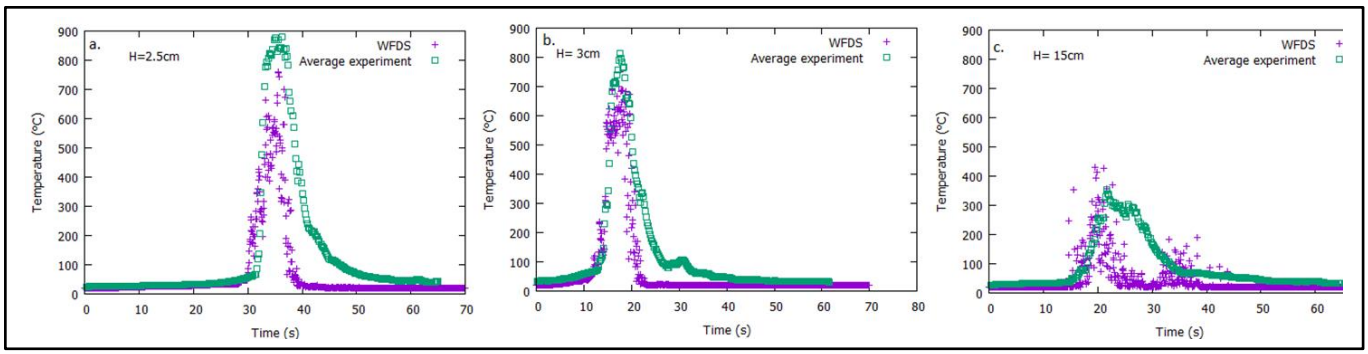

Figure 7: Comparison of temperature variation during burning between the WFDS modeling and the fuel bed burning experiments (mean values n= 2) at three different locations of the thermocouple: (a) H= 2.5 cm, (b) 3 cm, and (c) 15 cm.

In order to ensure the repeatability of measurements, the branch shapes were calibrated in each test for a given species and the thermocouples were located at the same positions around the branch. This approach allowed determining whether the temperatures captured in the modelling were the same as in the actual burnings. For the four species studied, numerical and experimental temperature variations during the branch burning were compared (Fig. 8), using the different sensors positioned around and above the branch (T_1, T_2 and T_3, Table 3). In Fig. 8*a* (oleander), the numerical and experimental data were in a good agreement, with a clear increase in temperature occurring at 33 s recorded by T_2, which was representative of the results obtained for this species. However, the modelling presented a supplementary peak at 25 s, which could be due to either the flame generated by the fuel bed itself or by an early ignition of the branch reaching the temperature sensor. The numerical and experimental maximum temperatures also differed slightly (on average 927°C for the experiments *v.* 827°C for the modelling) and the modelled temperature decreased steeply during the extinction phase. The result was the same for cotoneaster (Fig. 8*b*), with a peak of temperature beginning at 30 s in both simulation

and mean experiments and a 66°C difference between the two maximum temperatures. The decrease in temperatures remained fairly close for both curves, even if the decrease was slower during the extinction phase in the experiments, as previously explained for oleander. In this case, the data presented were recorded by T_1, which was representative of the results obtained for this species. For spindle (Fig. 8*c*), the simulated temperature variation (recorded by T_2) presented a plateau at ~450°C, between 40 and 50 s. This plateau was not present in the experiments but the curve presented a peak of 450°C at ~45 s. Then, as described before, the decrease in temperature was sharper in the simulation. Finally, for cypress (Fig. 8*d*), numerical and experimental temperature variations (recorded by T_3) presented a 10-s offset between the two temperature peaks but the increase in temperature began, in both cases, at 20 s and the maximum temperature reached 500°C (at 22 s in the simulation and 32 s in the mean experiments). Besides the slower decrease in temperatures in the experiments (mean values), a slight difference (<50°C) could also be observed during the extinction phase for which the predicted temperatures were lower than the experimental ones, regardless of species (up to 10% of the total temperature emitted during the experimental burnings of cypress).

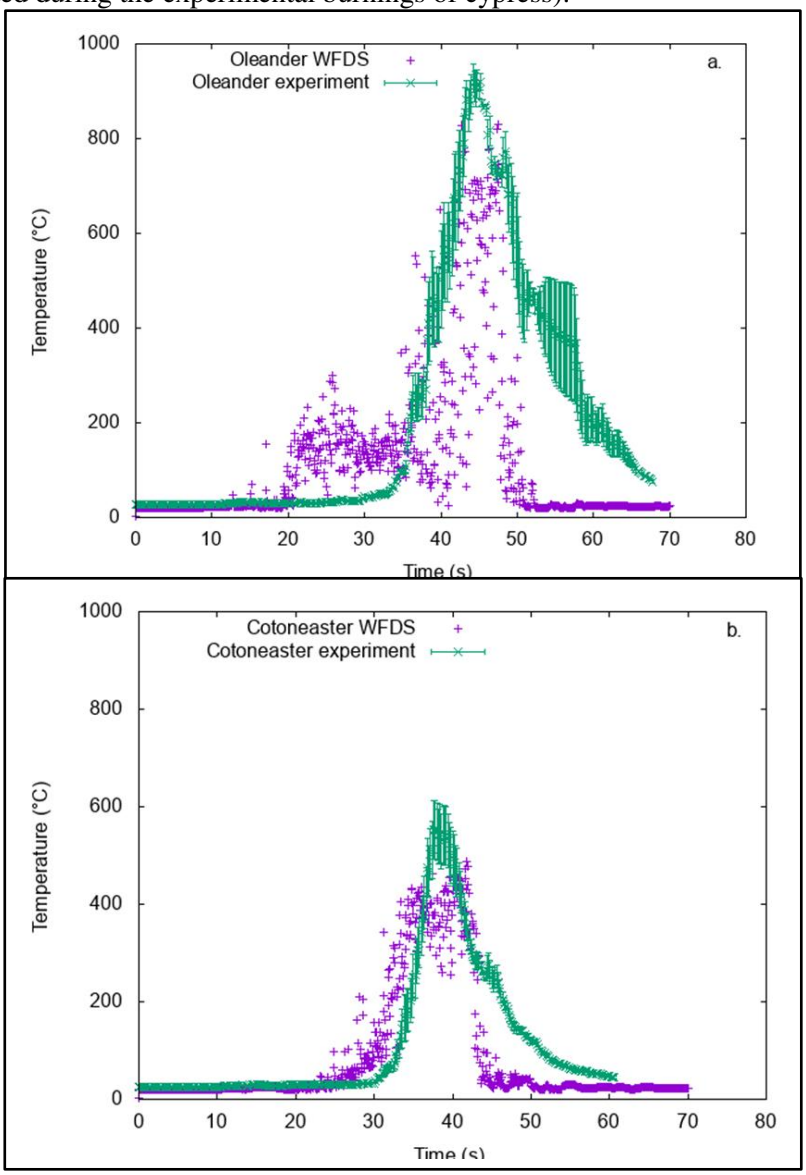

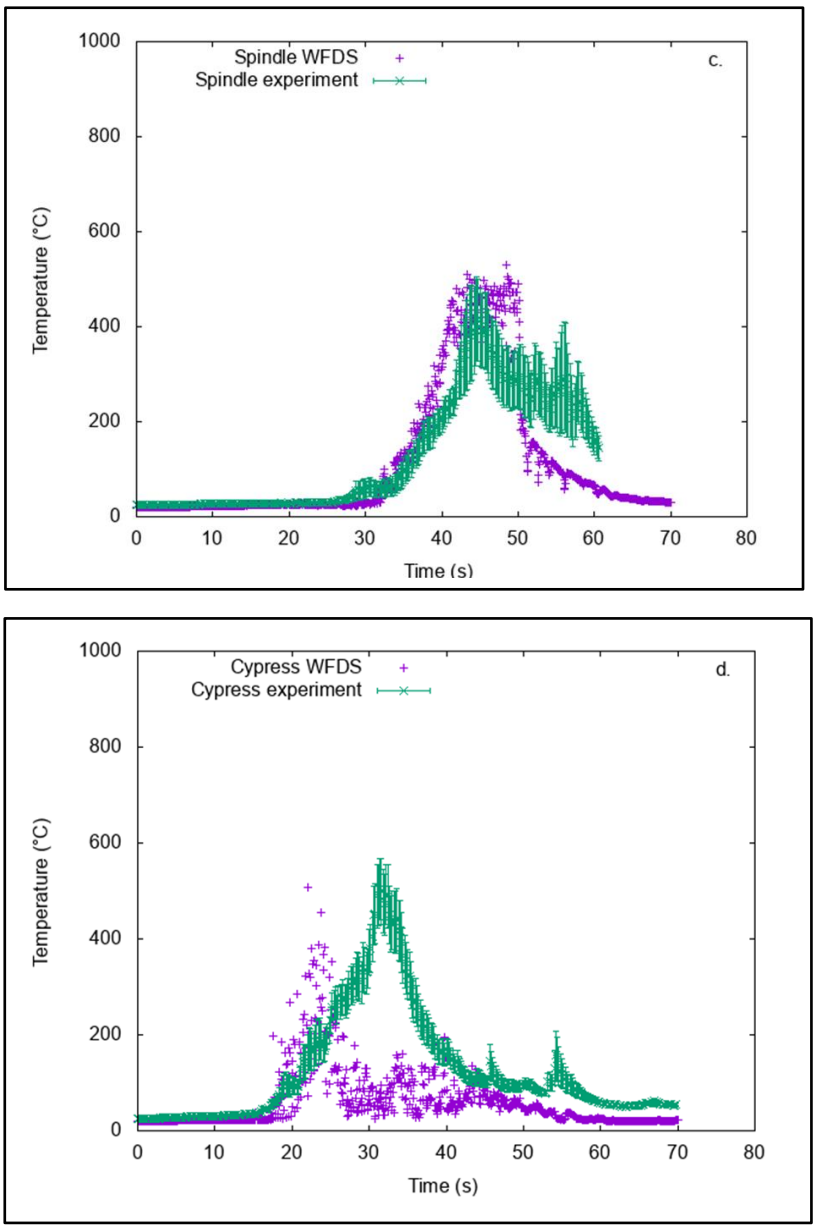

Figure 8: Comparison between modeling and experiments (mean values) regarding the variation of temperatures measured by three thermocouples during the burning of the branches of the four species: (a) oleander (b) cotoneaster, (c) spindle, (d) cypress (T_1= thermocouple 1 located above the branch, T_2= thermocouple 2 located to the left of the branch, T_3= thermocouple 3 located to the right of the branch).

Ranking of species according to their flammability

The flammability variables measured during the experiments and in the modelling (Table 4) were used to rank the four species according to their flammability (Fig. 9*a*, *b*). This also allowed us to check the rankings of species based on the experiments and on modelling differed. The comparison between both rankings highlighted the same groups of species: the first group was composed of cypress (Cy)

and oleander (Ol) whereas the second group comprised spindle (Sp) and cotoneaster (Co). The experimental results (Table 4 and Fig. 9*a*, *c*) showed that cypress and oleander were characterised by higher combustibility (regarding MeanMaxT) and consumability but by a contrasted ignitability with higher values of TTI but low value of IgT for cypress only. Spindle and cotoneaster also presented contrasted ignitability (short TTI but high IgT), sustainability (longer FD for cotoneaster contrary to spindle) and combustibility (higher ROS for spindle contrary to cotoneaster but lower MeanMaxT for both species). In the modelling, results were clearer (Table 4 and Fig. 9*b*, *d*), the first group (cypress and oleander) presenting higher combustibility and consumability but ignitability still contrasted (long TTI for both species but lower IgT for cypress). The second group (spindle and cotoneaster) was characterised by high sustainability, lower consumability and combustibility but a contrasted ignitability (short TTI but high IgT). On the whole, the group composed of cypress and oleander could be considered as more flammable than that of spindle and cotoneaster.

According to the type of ranking, the distance between cotoneaster and spindle was smaller in the modelling ranking than in the experimental one, meaning that these species were considered very similar in the modelling, as opposed to the experiments (Fig. 9*a*, *b*). In fact, the disparities between the numerical values were less important for cotoneaster and spindle than for the experimental values (for instance, regarding MeanMaxT: difference of 186°C in the experiments *v.* 48°C in the modelling, or regarding MLR: 0.04 g s^{-1} in the modelling *v.* 0.1 g s^{-1} in the experiments). In contrast, the distance between cypress and cotoneaster was smaller in the experimental ranking (differences between TTI, FD, MLR, for instance, were smaller in the experiments than in the modelling).

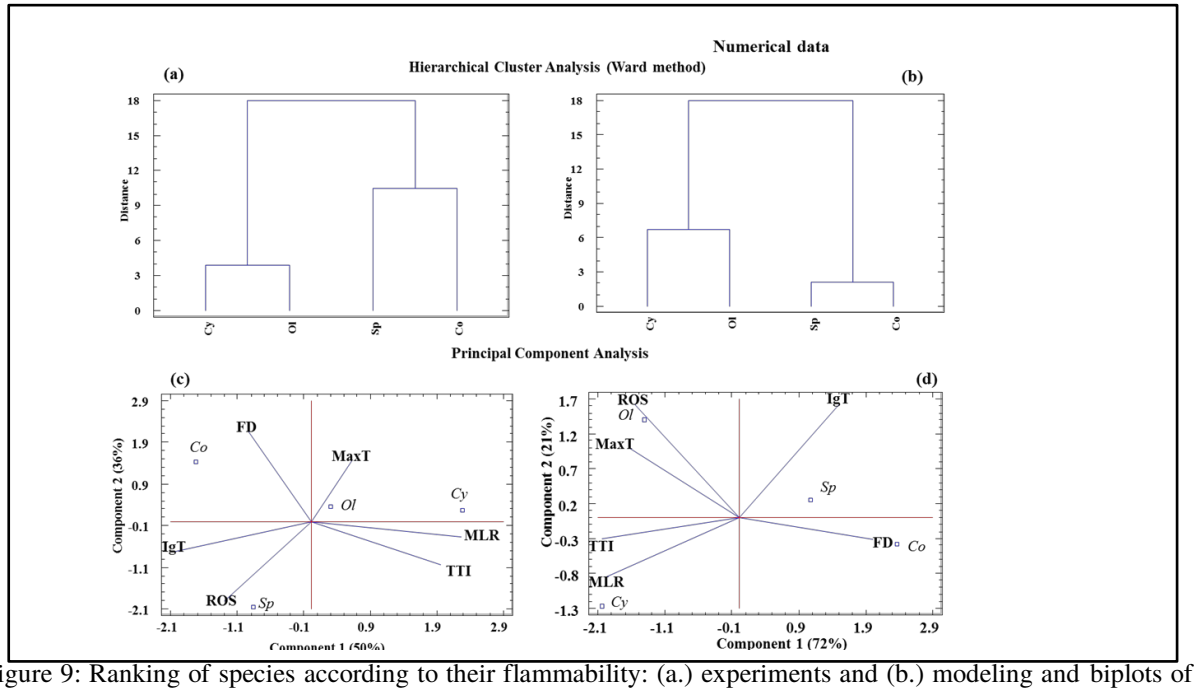

Figure 9: Ranking of species according to their flammability: (a.) experiments and (b.) modeling and biplots of principal component analysis showing relationships between the four species and flammability variables obtained in (c) experiments and (d) modeling (Cy: Cypress, Ol: Oleander, Sp: Spindle, Co: Cotoneaster, TTI:

time-to-ignition, IgT: ignition temperature, FD: flaming duration, MLR: mass loss rate,%bB: proportion of branch burned, MaxT: mean maximum temperature, ROS: rate of spread).

Discussion

Comparing results between burning experiments and modelling

The flammability variables recorded during the experiments and in the modelling were compared and differences were highlighted in some cases, in particular regarding the maximum temperature or the rate of spread. Regarding the different species, the most interesting point was that the branch mass was the same after burning experiments and modelling were complete, showing that mass losses could differ between species (especially for cypress and oleander) but that the final mass would be similar between the modelling and the experiments. At the modelling level, the major problem could be the simplified geometric definition of the branches; by contrast, the modelled fuel-bed burnings matched the experimental ones. Moreover, in most burnings, the branch was ignited as soon as the leaf was set on fire; for instance, the ignition of the cypress branch first took place at the level of the leaves located at the lowest part of the branch, therefore the closest to the flames. However, taking into account such a fine resolution in the branch geometric definition (i.e. modelling each leaf in WFDS) was not possible; the precise modelling of the ignition zone was impossible and, thus, were not correctly modelled. Indeed, WFDS uses only cylinders to model an equivalent homogeneous medium, meaning that, in a given cell, there is no distinction between wood, leaves and twigs. Hence, the ignition of a single leaf cannot be simulated with multiphase modes, such as WFDS, and ignition occurs in the simulations when the whole cell (wood, leaves and twigs) has ignited. Some of the differences between the modelling and the experimental results could also be explained by the possible random branch motion during the burning due to convection. This motion entailed a possible variation of the temperature sensed by the thermocouple which could not be modelled by WFDS as there was no appropriated modelling for the branch motion around its balance position. Despite this latter approximation, the simulation results seemed acceptable as in the works of Dupuy *et al.* (2011) and Pimont *et al.* (2011) who modelled crown fires neglecting the canopy movements during the fire.

Besides the flammability variables recorded, numerical and experimental variations of mass loss and temperatures over time have also been compared and showed a good agreement. Variations of temperatures were similar for the temperature sensors located close to the fuel bed but varied when the thermocouple was positioned farther above the fuel bed (at a height of 15 cm). In that case, the turbulent flame behaviour was more pronounced, influencing the simulated temperature measurements. Previous works on fuel-bed burning experiments carried out in laboratory conditions

showed data comparable to the WFDS modelling (Menage *et al*. 2012; Perez-Ramirez *et al*. 2017). However, there are few works dealing with the experimental propagation of the flame from the fuel bed to the branch (vertical propagation) and, then, through the branch (horizontal propagation) (e.g. Ganteaume *et al*. 2016), not to mention the modelling of this type of fire propagation. The modelling of the flame propagation from the fuel bed to the branch according to the branch moisture content showed that the mass loss over time only varied slightly (less than 1 g) for the highest FMC (25%), highlighting that the branch did not ignite in the simulation at this moisture content. This test allowed the confirmation of the choice of moisture content lower than 25% to be able to model the fire propagation at this scale using WFDS. Very few works dealt with the comparison of experimental and numerical fire behaviour in fuels with high FMC (i.e. values of FMC corresponding to live fuel are 100% on average, depending on species and season) as these works were mostly carried out on fuel beds of litter or grasses (Morvan and Dupuy 2001; Overholt *et al*. 2014*a*, 2014*b*; Perez-Ramirez *et al*. 2017). Even Mell *et al*. (2009) burned Douglas-firs of different heights whose moisture contents did not exceed 50% (which is far from the actual live FMC of this species), may be because of the difficulty to ignite entire trees with higher FMC. In the experiments, even with a moisture content of 25%, the flame propagated from the fuel bed to the branch and then through the branch, the excelsior fuel bed releasing enough heat to allow this vertical and horizontal propagation. In a previous work, Ganteaume *et al*. (2016) conducted burning experiments using branches with moisture contents that could exceed 100% and obtained successful ignition when the flame front propagated underneath the branches. By contrast, when the fuel bed was removed from underneath (such as was done when cleaning under an ornamental hedge, for instance), the flames did not propagate vertically very well and, in most cases, the branch did not sustain the horizontal flame propagation as the energy released only by the burning of a few leaves (or parts of leaves) was not sufficient.

Based on a visual inspection of the plots, the simulated temperature variation over time was, on the whole, in a good agreement with the experimental data, despite some minor discrepancies in some tests. For instance, regarding cypress, the experimental and numerical temperature variations over time recorded by the thermocouple 3 visually showed the same trend but the temperature peak was shifted in time (~10 s). This gap could be due to a faster ignition in the modelling entailed by a faster mass loss of the cypress branch. Moreover, the decrease in temperature was longer during the extinction phase in the experiments and this could be due, for instance, to the thermocouple sensitivity allowing the recording of the high temperature reached by the branch at the end of the burning (extinction phase) as the sensor was close to the burning branch. Overall, the results seemed to be fairly convincing despite the above-mentioned biases.

Comparing flammability rankings

The rankings of species according to their flammability were the same for the experiments and the modelling, highlighting two groups of contrasted flammability (the more flammable cypress and

oleander, mainly because of their higher combustibility and consumability, and the less flammable spindle and cotoneaster); the latter group would be considered as less problematic in case of fire in WUI. In both groups, the ignitability was contrasted, cypress and oleander presenting longer TTI but lower IgT (regarding cypress only, maybe because this species' leaves contain terpenes whose flash points are low) contrary to spindle and cotoneaster. A few works discussed the ranking of species according to the branch flammability and the species studied differed from those currently burned (Dimitrakopoulos 2001; Wyse *et al*. 2016). Moreover, none compared rankings obtained from modelling and experiments. Opinions on the species' flammability could vary according to previous works, which could differ in terms of methodology or fuel type studied. Regarding cypress, some works concluded that leaf samples were moderately flammable (Valette 1990; Ganteaume *et al*. 2013*b*) and even that this species could be used as a firewall (Della Rocca *et al*. 2015). By contrast, Dimitrakopoulos and Papaiannou (2001), as well as Liodakis *et al*. (2002), considered this species at leaf and ground sample scales among the most flammable species. Ganteaume *et al*. (2013*b*) agreed with this ranking but only regarding dead leaf samples. Likewise, the ranking also differed between previous works for oleander, ranked either as poorly flammable (Dimitrakopoulos 2001; Long *et al*. 2006) or as very flammable (Ganteaume *et al*. 2013*b*). Dimitrakopoulos (2001) also highlighted a variation of flammability between branches and leaves of different species, leaves being more flammable than branches. In the current work, the rankings were obtained using branches whose FMC was lower than 25% for all species. Given the important role of this parameter on flammability (Chuvieco *et al*. 2004), it was crucial to avoid any moisture content variation between the tests. However, other fuel characteristics can influence the plant flammability, such as leaf thickness (Montgomery and Cheo 1971; Ganteaume *et al*. 2016; Ganteaume 2018). The difference between rankings could also be explained by the type of fuel bed used to generate the flame front. In similar works, the fuel bed used was that of the species studied, so differed between species (Montgomery and Cheo 1971; Ganteaume *et al*. 2016), which is in contrast to the current work in which the fuel bed was the same (i.e. excelsior) for the different species. In future works, experimental and numerical approaches of the fire behaviour in ornamental vegetation will have to be extended to entire plants and groups of plants in order to have a broader and more accurate picture of the issue of such flammable species in WUI, especially species containing huge amount of dead fuel within their canopy such as *Cupressus sempervirens* var. *fastigiata*.

Experiment and modelling limitations

At the experimental level, drying the branch in a closed chamber without controlling the environmental parameters is a technique needing improvements (even in a closed environment, relative humidity and temperature still slightly vary especially when the meteorological conditions change). Indeed, according to this approach, drying was not homogeneous, in particular for the oleander branches, which presented the largest leaves. A climatic chamber that would allow adjusting

the humidity and the temperature during the drying would be the best option as the different species would be air-dried according to the same climatic conditions. Moreover, even if the excelsior fuel bed (that presented the same parameters from one burning to the other) burned homogeneously, its distribution on the fire bench could not be completely identical from one burning to the other (due to the structure of the excelsior). This could affect the flame front; hence, the exact spot of the branch ignition. Of course, the possible variability in the experiments, i.e. due to the motion of the branches generated by convection during the burning, should also be taken into account, for example, through the standard deviations around the mean experimental values.

At the level of the WFDS modelling, one of the major issues was the geometric definition of the branch, using only cylinders oriented in one direction, which limited the accuracy of the geometry. To overcome this problem, the branches were elaborated with a high number of cylinders of different sizes, representing the equivalent homogeneous medium. However, the experiments showed that the branch ignition could be due to the ignition of only one leaf and modelling this phenomenon was not possible, especially because the size of a cylinder differed from that of a leaf. Indeed, this size had to correspond to a representative elementary volume of a branch. In future works, the branch geometry should be modelled with the more efficient FUEL 3D to observe the effect of the geometry on the branch ignition and combustion.

Conclusions

The purpose of this work was to model the flame propagation from the fuel bed to the branch, then in the branch of four ornamental species using the WFDS software and to compare numerical and experimental results. The four species studied presented different branch geometries, leaf shapes, and biomasses; therefore a large number of plant characteristics had to be taken into account in these comparisons., In general, they showed a good agreement (magnitude of differences often lower than 25%), despite some biases in both modelling and experiments.

The numerical and experimental mass losses during burnings were in agreement, time to ignition often varying but the final masses being the same. Differences in temperatures were mostly due to the modelling limitations (small particles likely to ignite during the experiment and that could not be generated by WFDS) and to the experimental variability (such as branch motion due to convection or longer decrease in temperature due to the high sensitivity of thermocouples). For each species, the modelling of the branches was based on coarse shapes that were, however, finer than the basic shapes used in the WFDS modelling. Moreover, results showed that the modelled branch burning occurred only when FMC was lower than 25%, whereas the critical FMC in ornamental vegetation, in summer, is at least 60% for some ornamental species (Ganteaume 2018). Beyond that point, the plant is often considered as dead (Pellizzaro *et al*. 2007), meaning that the modelling using FMC lower than 25% was a first step in attempting the modelling of fire propagation but did not reflect the reality of live

fuels, even in case of severe drought. Consequently, the most important point would be to improve the modelling for moisture content higher than 60% (i.e. live plants) in adopting a multiphase model for live plants such as suggested in Lamorlette *et al*. (2018).

Despites these limitations, the flammability ranking of the four species studied did not differ between the WFDS modelling and the experiments. Both rankings highlighted the same two groups of species; cypress and oleander being the most flammable, suggesting that this type of study could be conducted using mainly numerical means, however, as stated in previous works (Ganteaume *et al*. 2013*b*; Ganteaume 2018), in the future, the work has to be carried out at a larger scale (i.e. at the level of the entire plant) for a better accuracy of the flammability assessment and, thus, of the fire risk assessment in WUI.

Conflicts of interest

The authors declare that they have no conflicts of interest.

Declaration of funding

This research did not receive any specific funding.

Acknowledgements

The authors thank the Irstea's technical staff, Roland Estève, Fabien Guerra, Christian Travaglini and Jean-Michel Lopez, for their contribution in the field and in the laboratory during the burning experiments. The authors also sincerely thank William (Ruddy) Mell for his valuable comments on this work and Aimee Mac Cormack for English revision.

References

Anderson HE (1970) Forest fuel ignitibility. *Fire Technology* **6**, 312–319. doi:10.1007/BF02588932

Bear J, Bachmat Y (2012) 'Introduction to Modeling of Transport Phenomena in Porous Media. Vol. 4.' (Springer Science & Business Media)

Bufacchi P, Krieger GC, Carvalho JA (2016) Numerical simulation of surface forest fire in Brazilian Amazon. *Fire Safety Journal* **79**, 44–56. doi:10.1016/j.firesaf.2015.11.014

Castle DC (2015) 'Numerical modeling of laboratory-scale surface-to-crown fire transition. PhD thesis, San Diego State University, San Diego, USA.

Castle D, Mell WE, Miller FJ (2013) Examination of the wildland–urban interface fire dynamics simulator in modeling of laboratory-scale surface-to-crown fire transition. 8th U.S. Nat Combust Meet, May 19-22, 2013, Combustion Institute, Park City, UT,, USA, pp 3710-3722, Curran Associates, Inc. , Red Hook, NY

Chuvieco E, Aguado I, Dimitrakopoulos AP (2004) Conversion of fuel moisture content values to ignition potential for integrated fire danger assessment. *Canadian Journal of Forest Research* **34**, 2284–2293. doi:10.1139/x04-101

Chuvieco E, González I, Verdú F, Aguado I, Yebra M (2009) Prediction of fire occurrence from live fuel moisture content measurements in a Mediterranean ecosystem. *International Journal of Wildland Fire* **18**(4), 430–441. doi:10.1071/WF08020

Cobian-Iñiguez J, Aminfar A, Chong J, Burke G, Zuniga A, Weise DR, Princevac M (2017) Wind tunnel experiments to study chaparral crown fires. *Journal of Visualized Experiments* **139**, e56591. doi:10.3791/56591.

Della Rocca G, Pecchioli A, Moya B (2015) Possible land management uses of common cypress to reduce wildfire initiation risk: a laboratory study. *Journal of Environmental Management* **159**, 68–77. doi:10.1016/j.jenvman.2015.05.020

Dickinson MB, Johnson EA, Artiaga R (2013) Fire spread probabilities for experimental beds composed of mixedwood boreal forest fuels. *Canadian Journal of Forest Research* **43**, 321–330. doi:10.1139/cjfr-2012-0291

Dimitrakopoulos AP (2001) A statistical classification of Mediterranean species based on their flammability components. *International Journal of Wildland Fire* **10**, 113–118. doi:10.1071/WF01004

Dimitrakopoulos AP, Papaioannou KK (2001) Flammability assessment of Mediterranean forest fuels. *Fire Technology* **37**, 143–152. doi:10.1023/A:1011641601076

Dupuy JL, Linn R, Konovalova V, Pimont F, Vega JA, Jiménez E (2011) Exploring three-dimensional coupled fire-atmosphere interactions downwind of wind-driven surface fires and their influence on backfires using the HIGRAD-FIRETEC model. *International Journal of Wildland Fire* **20**, 734–750. doi:10.1071/WF10035

El Houssami M (2016) Development of a numerical and experimental framework to understand and predict the burning dynamics of porous fuel beds. PhD thesis, University of Edinburgh, Edinburgh, UK.

El Houssami M, Thomas JC, Simeoni A (2016) Experimental and numerical studies characterizing the burning dynamics of wildland fuels. *Combustion and Flame* **168**, 113–126. doi:10.1016/j.combustflame.2016.04.004

El Houssami M, Lamorlette A, Morvan D, Hadden RM, Simeoni A (2018) Framework for submodel improvement in wildfire modeling. *Combustion and Flame* **190**, 12–24. doi:10.1016/j.combustflame.2017.09.038

Etlinger MG, Beall FC (2004) Development of a laboratory protocol for fire performance of landscape plants. *International Journal of Wildland Fire* **13**, 479–488. doi:10.1071/WF04039

Ganteaume A (2018) Does plant flammability differ between leaf and litter bed scale? Role of fuel characteristics and consequences for flammability assessment. *International Journal of Wildland Fire* **27**, 342–352. doi:10.1071/WF17001

Ganteaume A, Long-Fournel M (2015) Driving factors in fire density can spatially vary at the local scale in south-eastern France. *International Journal of Wildland Fire* **24**, 650–664. doi:10.1071/WF13209

Ganteaume A, Jappiot M, Lampin C (2013*a*) Assessing the flammability of surface fuels beneath ornamental vegetation in wildland–urban interfaces in Provence (south-eastern France). *International Journal of Wildland Fire* **22**, 333–342. doi:10.1071/WF12006

Ganteaume A, Jappiot M, Hernando C (2013*b*) Flammability of some ornamental species in wildland–urban interfaces in southeastern France: laboratory assessment at particle level. *Environmental Management* **52**, 467–480. doi:10.1007/s00267-013-0067-z

Ganteaume A, Bertin A, Audouard M, Guerra F, Lopez JM, Morge D, Travaglini C, Jappiot M (2016) How ornamental vegetation burns: from particle flammability to vertical flame propagation. In 'ForestFire 2016: International Conference on Forest Fires and WUI Fires', 25–27 May 2016, Aix-en-Provence, France.

Grishin A (1997) 'Mathematical Modeling of Forest Fires and New Methods of Fighting Them.' (Ed. F Albini) (Tomsk State University: Tomsk, Russia)

Hoffman C, Morgan P, Cook S (2012) Numerical simulation of crown fire hazard immediately after bark beetle-caused mortality in lodgepole pine forests. *Forest Science* **58**, 178–188. doi:10.5849/forsci.10-137

Lamorlette A, Candelier F (2015) Thermal behavior of solid particles at ignition: theoretical limit between thermally thick and thin solids. *International Journal of Heat and Mass Transfer* **82**, 117–122. doi:10.1016/j.ijheatmasstransfer.2014.11.037

Lamorlette A, El Houssami M, Morvan D (2018) An improved non-equilibrium model for the ignition of living fuel. *International Journal of Wildland Fire* **27**(1), 29–41. doi:10.1071/WF17020

Liodakis S, Bakirtzis D, Lois E (2002) TG and autoignition studies on forest fuels. *Journal of Thermal Analysis and Calorimetry* **69**, 519–528. doi:10.1023/A:1019907706137

Long AJ, Behm A, Mell W (2006) Quantifying and ranking the flammability of ornamental shrubs in the southern United States. In '2006 Fire Ecology and Management Congress Proceedings' DVD).' (The Association for Fire Ecology/ Washington State University Extension: San Diego, CA) dates, location. (Eds) pp. 13–17. (publisher: publication location)

Martin RE, Gorden DA, Gutierrez ME, Lee DS, Molina DM, Schroeder RA, Sapsis DA, Stephens SL, Chambers M (1993) Assessing the flammability of domestic and wildland vegetation. In 'Proceedings of the 12th Conference on Fire and Forest Meteorology', 26–28 October 1993, Jekyll Island, GA, USA. (Eds) pp. 130–137. (publisher: publication location)

McGrattan K, Hostikka S, McDermott R, Floyd J, Weinschenk C, Overholt K (2013) Fire Dynamics Simulator user's guide. National Institute of Standards and Technology, Technical Report NIST Special Publication 1019–6. (Gaithersburg, MD, USA)

Mell W (2010). User Guide to WFDS. Wildland-urban interface Fire Dynamics Simulator. San Francisco.

Mell W, Gould J, Cheney P (2007) A physics-based approach to modelling grassland fires. *International Journal of Wildland Fire* **16**, 1–22. doi:10.1071/WF06002

Mell W, McDermott R, Manzello SL (2009) Numerical simulation and experiments of burning Douglas-fir trees. *Combustion and Flame* **156**, 2023–2041. doi:10.1016/j.combustflame.2009.06.015

Mell W, McDermott RJ, Forney GP (2010) Wildland fire behavior modeling: perspectives, new approaches and applications. In 'Proceedings of 3rd Fire Behavior and Fuels Conference', Oct. 25-29, 2010, Spokane, WA, USA. (Eds) p. 45. . (publisher: publication location)

Menage D, Chetehouna K, Mell W (2012) Numerical simulations of fire spread in a *Pinus pinaster* needles fuel bed. *Journal of Physics* **395**(1), 012011. doi:10.1088/1742-6596/395/1/012011

Monod B, Collin A, Parent G, Boulet P (2009) Infrared radiative properties of vegetation involved in forest fires. *Fire Safety Journal* **44**(1), 88–95. doi:10.1016/j.firesaf.2008.03.009

Montgomery KR, Cheo PC (1971) Effect of leaf thickness on ignitibility. *Forest Science* **17**, 475–478.

Morvan D, Dupuy JL (2001) Modeling of fire spread through a forest fuel bed using a multiphase formulation. *Combustion and Flame* **127**, 1981–1994. doi:10.1016/S0010-2180(01)00302-9

Nepf HM (1999) Drag, turbulence, and diffusion in flow through emergent vegetation. *Water Resources Research* **35**(2), 479–489. doi:10.1029/1998WR900069

Overholt KJ, Kurzawski AJ, Cabrera J, Koopersmith M, Ezekoye OA (2014a) Fire behavior and heat fluxes for lab-scale burning of little bluestem grass. *Fire Safety Journal* **67**, 70–81. doi:10.1016/j.firesaf.2014.05.007

Overholt KJ, Cabrera J, Kurzawski AJ, Koopersmith M, Ezekoye OA (2014b) Characterization of Fuel Properties and Fire Spread Rates for Little Bluestem Grass *Fire Technology*, 50, 9-38

Parsons RA, Mell WE, McCauley P (2011) Linking 3D spatial models of fuels and fire: effects of spatial heterogeneity on fire behavior. *Ecological Modelling* **222**(3), 679–691. doi:10.1016/j.ecolmodel.2010.10.023

Pellizzaro G, Duce P, Zara P (2007) Seasonal variations of live moisture content and ignitability in shrubs of the Mediterranean Basin. *International Journal of Wildland Fire* **16**, 633–641. doi:10.1071/WF05088

Perez-Ramirez Y, Mell WE, Santoni PA, Tramoni J-B, Bosseur F (2017) Examination of WFDS in modeling spreading fires in a furniture calorimeter. *Fire Technology* **53**(5), 1795–1832. doi:10.1007/s10694-017-0657-z

Pimont F, Dupuy JL, Linn R, Dupont S (2011) Impacts of tree canopy structure on wind flows and fire propagation simulated with FIRETEC. *Annals of Forest Science* **68**(3), 523–530. doi:10.1007/s13595-011-0061-7

Prince DR, Fletcher ME, Shen C, Fletcher TH (2014) Application of L-systems to geometrical construction of chamise and juniper shrubs. *Ecological Modelling* **273**, 86–95. doi:10.1016/j.ecolmodel.2013.11.001

Syphard AD, Radeloff VC, Hammer RB (2007) Human influence on California fire regimes. *Ecological Applications* **17**, 1388–1402. doi:10.1890/06-1128.1

Valette J-C (1990) Inflammabilités des espèces forestières méditerranéennes Conséquences sur la combustibilité des formations forestières. *Revue Forestière Française* **42**, 76–92. doi:10.4267/2042/26171

Wishart D (1969) 256 Note: An algorithm for hierarchical classifications. *Biometrics* **25**, 165–170. doi:10.2307/2528688

Wyse SV, Perry GLW, Curran TJ (2016) A quantitative assessment of shoot flammability for 60 tree and shrub species supports rankings based on expert opinion. *International Journal of Wildland Fire* **25**, 466–477. doi:10.1071/WF15047

Ziegler JP, Hoffman C, Battaglia M, Mell W (2017) Spatially explicit measurements of forest structure and fire behavior following restoration treatments in dry forests. *Forest Ecology and Management* **386**, 1–12. doi:10.1016/j.foreco.2016.12.002

TABLES

Table 1. Fuel bed parameters used as inputs in WFDS (Wildland–Urban Interface Fire Dynamical Simulator)

Parameters	Value	Reference
Fuel bed width (cm)	30	Set value
Fuel bed length (cm)	40	Set value
Fuel bed depth (cm)	1.5	Set value
Fuel bed mass (g)	15	Set value
Moisture (g g^{-1})	0.06 ± 0.02	Measured
Initial temperature (°C)	20	Default in WFDS
Surface area-to-volume ratio (m^{-1})	8810 ± 446	Measured
Char fraction (g g^{-1})	0.25	Default in WFDS
Drag coefficient (–)[A]	0.375	(Mell 2010; Nepf 1999)
Leaf density (kg m^{-3})	633.83 ± 113	Measured
Bulk density (kg m^{-3})	8.33 ± 1.2	Measured
Burning rate (kg $m^{-3}.s^{-1}$)	1 ± 0.07	Measured
Dehydration rate (kg m^{-3} s^{-1})	0.4	Default in WFDS

[A]The variation of the branch drag coefficient is not significant regarding the particle sizes and flow velocities characterising the experiments; i.e. Nepf 1999).

Table 2. Branch parameters (average ± standard deviation) used in WFDS (Wildland–Urban Interface Fire Dynamical Simulator)

Parameters	Cotoneaster	Cypress	Spindle	Oleander	Reference
Width (cm)	34 ± 5	22 ± 3.8	29 ± 5	28.5 ± 1	Measured
Length (cm)	25 ± 6	13 ± 1	18 ± 2.8	19 ± 3	Measured
Depth (cm)	6 ± 4	4 ± 1.8	8 ± 2	5.5 ± 1	Measured
Mass (g)	10 ± 3.3	18.4 ± 0.8	14.4 ± 1.5	25.7 ± 3.3	Measured
Moisture (g g^{-1})	0.1 ± 0.04	0.18 ± 0.03	0.2 ± 0.02	0.18 ± 0.04	Measured
Initial temperature (°C)	20	20	20	20	Default in WFDS
Surface area-to-volume ratio (m^{-1})	3655 ± 351	3670 ± 493.3	4720 ± 955	2278 ± 360.5	Measured
Char fraction (g g^{-1})	0.3 ± 0.06	0.3 ± 0.02	0.3 ± 0.04	0.3 ± 0.1	Measured
Drag coefficient (–)[A]	0.375	0.375	0.375	0.375	(Mell 2010; Nepf 1999)
Leaf density (kg m^{-3})	329.26 ± 150	1251.23 ± 960	903.06 ± 80	933 ± 80	Measured
Bulk density (kg m^{-3})	2.9 ± 1	9 ± 1.1	5.36 ± 1.3	7.3 ± 1.6	Measured
Burning rate (kg $m^{-3}.s^{-1}$)	0.07 ± 0.06	0.54 ± 0.06	1 ± 0.3	0.9 ± 0.11	Measured
Dehydration rate (kg m^{-3} s^{-1})	0.4	0.4	0.4	0.4	Default in WFDS
Heat of combustion (kJ kg^{-1})	17700	17700	17700	17700	Default in WFDS
Number of cylinders	95	22	73	161	–
Number of tests	6	8	7	3[B]	–

[A]The variation of the branch drag coefficient is not significant regarding the particle sizes and flow velocities characterising the experiments, i.e. Nepf (1999).

[B]The lower number of replicates for oleander was due to problems during the heterogeneous air-drying of some branch samples that were discarded.

Table 3. Locations of the three thermocouples in the experiments and the modelling for the four species studied (Cartesian system presented in Fig. 1*a*)

	Thermocouple 1			Thermocouple 2			Thermocouple 3		
Location in Cartesian system	$\vec{x}$	$\vec{y}$	$\vec{z}$	$\vec{x}$	$\vec{y}$	$\vec{z}$	$\vec{x}$	$\vec{y}$	$\vec{z}$
Cypress	19.5	11	17	21	14	19	25	13	25
Spindle	15	13.5	15	22.5	15	21	21	15	31
Cotoneaster	23	10	16	22.5	19	17	24	13.5	21
Oleander	20	13	21.5	32.5	15.5	22	21.5	17	37

Table 4. Flammability variables measured during the burning experiments (mean ± standard deviation) and obtained in modelling for the four species studied

Experimental ignition temperature was used as input data in the modelling. The magnitude of the difference between experimental and simulated values were given (except for MeanMaxT) when the simulated value was out of the range given by the standard deviation (TTI, time to ignition; IgT, ignition temperature; FD, flame duration; %bB, proportion of burned branches; MLR, mass loss rate; $MaxT_1$, maximum temperature measured by thermocouple 1; $MaxT_2$, maximum temperature measured by thermocouple 2; $MaxT_3$, maximum temperature measured by thermocouple 3; MeanMaxT, average on $MaxT_{1–3}$; ROS, rate of spread)

Flammability component	Flammability variable		Cypress	Spindle	Cotoneaster	Oleander
Ignitability	TTI (s)	Average experiment	30 ± 4	26 ± 3	17 ± 4	28 ± 5
		Modelling	37	26	17	31
		Magnitude of the difference (%)	18.9	-	-	-
	IgT (°C)	Average experiment	248.8 ± 40	263.7 ± 42	261 ± 32	260.5 ± 9
		Modelling	248.8	263.7	261	260.5
		Magnitude of the difference (%)	-	-	-	-
Sustainability	FD (s)	Average experiment	33 ± 5	28 ± 5	44 ± 4	35 ± 5
		Modelling	18	24	34	19
		Magnitude of the difference (%)	-45.5	-	-22.7	-45.7
Consumability	MLR ($g\ s^{-1}$)	Average experiment	0.37 ± 0.1	0.18 ± 0.04	0.08 ± 0.01	0.21 ± 0.1
		Modelling	0.68	0.14	0.1	0.9
		Magnitude of the difference (%)	45.6	-	20	-76.7
Combustibility	$MaxT_1$ (°C)	Average experiment	631 ± 62	323 ± 83	553 ± 57	733 ± 101
		Modelling	844	459	487	728
		Magnitude of the difference (%)	25.2	29.6	-11.9	-
	$MaxT_2$ (°C)	Average experiment	627 ± 50	416 ± 51	520 ± 100	927 ± 87
		Modelling	643	531	536	827
		Magnitude of the difference (%)	-	21.6	-	-10.8
	$MaxT_3$ (°C)	Average experiment	504 ± 57	445 ± 40	669 ± 73	789 ± 59
		Modelling	507	527	640	817
		Magnitude of the difference (%)	-	15.6	-	-

MeanMaxT (°C)	Average experiment	587 ± 72	395 ± 64	581 ± 78	816 ± 100
	Modelling	665 ± 169	506 ± 40	554 ± 78	791 ± 54
ROS (cm s^{-1})	Average experiment	0.67 ± 0.07	1.03 ± 0.1	0.77 ± 0.07	0.81 ± 0.04
	Modelling	1.22	1.21	1	1.5
	Magnitude of the difference (%)	45.1	14.9	23	46.7

.